DOI: 10.1002/ejic.200801259

Synthesis, Spectroscopic Properties and Electrochemical Oxidation of Ru^{II}-Polypyridyl Complexes Attached to a Peptide Nucleic Acid Monomer Backbone

Nickita Nickita,[a] Gilles Gasser,[a] Alan M. Bond,[a] and Leone Spiccia*[a]

Keywords: Ruthenium / Peptide nucleic acids / Synthesis / Electrochemistry / Electronic and emission spectroscopy

Monomeric *p*eptide *n*ucleic *a*cid (PNA) derivatives incorporating $[Ru(bpy)_2(Mebpy\text{-}PNA\text{-}OH)](PF_6)_2$ (**M1**) and $[Ru(bpy)_2(Mebpy\text{-}(CH_2)_4\text{-}PNA\text{-}OH)](PF_6)_2$ (**M2**), where bpy = 2,2′-bipyridine, Mebpy-PNA-OH = 2-[*N*-(2-{[(9*H*-fluoren-9-yl)methoxy]carbonylamino}ethyl)-4-methyl-2,2′-bipyridin-4′-ylcarboxamido]acetic acid and Mebpy-$(CH_2)_4$-PNA-OH = 2-[(2-{[(9*H*-fluoren-9-yl)methoxy]carbonylamino}ethyl){[5-(4-methyl-2,2′-bipyridin-4′-ylcarboxamido)pentyl]carbonyl}-amino]acetic acid, have been synthesised and characterised by IR and ^1H NMR spectroscopy, mass spectrometry and elemental analysis. $[Ru(bpy)_2(Mebpy\text{-}(CH_2)_4\text{-}COOH)](PF_6)_2$ (**4**) where Mebpy-$(CH_2)_4$-COOH = (4-methyl-2,2′-bipyridin-4′-yl)hexanoic acid, has been prepared as part of the multi-step conversion of $[Ru(bpy)_2(Mebpy\text{-}COOH)](PF_6)_2$ (**1**) to **M2**, as have *tert*-butyl ester precursors of **M1** and **M2**, $[Ru(bpy)_2(Mebpy\text{-}PNA\text{-}OC(CH_3)_3)](PF_6)_2$ (**2**) and $[Ru(bpy)_2(Mebpy\text{-}(CH_2)_4\text{-}PNA\text{-}OC(CH_3)_3)](PF_6)_2$ (**5**). ^1H NMR spectroscopy showed that **M1** and **M2** are present as rotamers in a 3:1 and 3:2 ratio, respectively. The UV/Vis spectra of **1**, **2**, **4**, **5**, **M1** and **M2** display a MLCT band at 452–454 nm. The emission maximum of **M1** in acetonitrile, detected on excitation at 450 nm, was slightly red-shifted compared to the emission of **M2** (622 nm), **1** (623 nm) and $[Ru(bpy)_3]^{2+}$ (615 nm). The Ru^{II}/Ru^{III} redox centers in **2**, **4** and **5** have $E°_f$ (reversible potentials) of +857 mV, +884 mV and +901 mV, respectively, vs. the $Fc^{0/+}$ (Fc = ferrocene) couple as determined from voltammetric studies in CH_3CN (0.1 M nBu_4NPF_6). Cleavage of the *tert*-butyl groups in **2** and **5** forms **M1** and **M2** whose $E°_f$ values lie at +908 mV and +895 mV vs. $Fc^{0/+}$ respectively, similar to those reported for **1** (+914 mV vs. $Fc^{0/+}$) and $[Ru(bpy)_3]^{2+}$ (+888 mV vs. $Fc^{0/+}$). A shift in the $E°_f$ of –57 mV was observed between **2** and **M1**, but little difference was detected **5** and **M2**, presumably due to the presence of a linker group in this latter case.

Introduction

*P*eptide *n*ucleic *a*cids (PNAs) are non-natural DNA mimics, which hybridise with complementary DNA/RNA strands by Watson–Crick base pairing.[1] Due to their neutral peptide backbone, which avoids electrostatic repulsions with negatively charged DNA/RNA strands, PNA-DNA/PNA-RNA duplexes are more stable than the usual DNA-DNA/RNA-RNA duplexes.[2] Another important feature of PNAs is their resistance to attack by proteases and nucleases.[2] Due to these favourable properties, the use of PNAs has been investigated for antisense[3–9] and antigene therapies.[10–14] Furthermore, the high selectivity of PNAs to detect even single RNA or DNA mismatches, has led their use in the biosensing area.[15–18] For this purpose, PNA-metal conjugates are particularly useful as they can act as electroactive and/or photoactive probes. Due to its well-established chemistry, availability, reversible electrochemistry and chemical stability,[19,20] ferrocene has been coupled to PNA monomers[21–29] or sequences.[30–32] Ferrocene, however, exhibits only electrochemical and no excited-state properties, in comparison to metal complexes, such as polypyridyl-Ru^{II} complexes, which feature both electrochemical and photochemical properties that can be utilised in biosensing. Metzler-Nolte et al. reported the synthesis of a Ru^{II} complex attached to a PNA monomer,[23] bis(bipyridyl)(4-methyl-4′-carboxylic acid bipyridyl)ruthenium(II) thymine-PNA methyl ester [Ru-(T-PNA)-OMe]. The Ru^{II}-PNA monomer exhibited a reversible oxidation process at 897 mV vs. $Fc^{0/+}$ and overlapping MLCT bands from 430–450 nm.[23] Subsequently, the same group described the attachment of a tris(bipyridine) Ru^{II} complex to a PNA heptamer where the metal centre had been inserted to the amino end of the sequence by automated synthesis.[32] On hybridisation of this Ru^{II}-bearing PNA heptamer with a complementary DNA strand, the CD (circular dichroism) spectra showed a positive Cotton effect by a shift in the maximum from 266 nm (PNA.DNA bioconjugate) to 280 nm (Ru-PNA-DNA bioconjugate).[32] Metal-containing

[a] School of Chemistry, Monash University,
Wellington Road, 3800 Clayton Victoria, Australia
Fax: +61-3-9905-4597
E-mail: Leone.Spiccia@sci.monash.edu.au
Supporting information for this article is available on the WWW under http://www.eurjic.org or from the author.

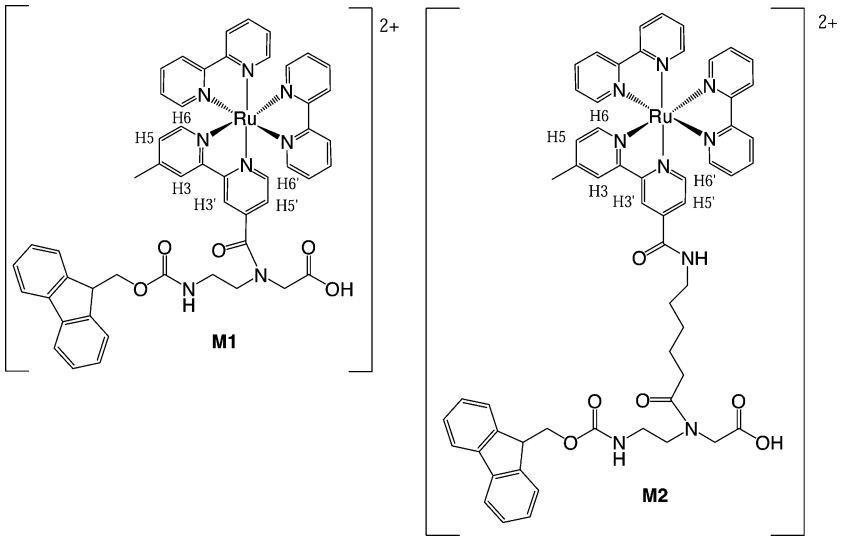

Figure 1. Monomeric PNA derivatives incorporating a Ru^{II} complex. Labels for proton assignments are included.

PNAs have also been synthesised by Achim et al. for purposes that include investigation of the electron transfer within PNA[33] and the increase in PNA-DNA stability through metal binding.[34]

In an effort to enhance the versatility of insertion of Ru^{II} complexes into PNAs, our group has envisaged an alternative approach involving the preparation of robust Ru^{II} complexes attached to the PNA backbone, which could be then inserted into a specific site within a PNA sequence. In contrast to the previous reports by Achim et al.,[34–36] who described the synthesis and then incorporation of bipyridine- and 8-hydroxyquinoline-containing PNA monomer into a PNA sequence, our aim is to insert the metal complex directly into the PNA sequence. For similar reasons, our approach is also different to that recently described by Gasser, Metzler-Nolte and co-workers who first inserted one or two alkyne-containing PNA monomers into PNA oligomers and then successfully applied "click chemistry" to attach ferrocene to these sequences.[30]

In this paper, the synthesis of monomeric PNA derivatives incorporating Ru^{II} complexes, **M1** and **M2**, (Figure 1) is described in which the DNA nucleobase found in a typical PNA monomer has been replaced by a Ru^{II} complex. **M1** from **M2** differ in the presence of a linker between the complex and the PNA backbone. ^{1}H NMR, luminescence and electrochemical characterisation are presented and compared to the starting material, $[Ru(bpy)_2(bpy\text{-}COOH)](PF_6)_2$ (**1**) to provide an understanding of substituent effects.

Results and Discussion

Synthesis and Characterisation

The synthetic routes toward **M1** and **M2** are described in Scheme 1. The known compound, $[Ru(bpy)_2(bpy\text{-}COOH)]^{2+}$ (**1**),[37] was chosen as the key synthon for the synthesis of two Ru^{II}-incorporated PNA monomers, **M1** and **M2**. The first step in the synthesis of **M1** involved the coupling of **1** to the PNA backbone, *tert*-butyl *N*-[2-(*N*-9-fluorenylmethoxycarbonyl)aminoethyl]-*N*-[(thymin-1-yl)acetyl]glycinate[38] to generate **2**. The conditions were similar to those reported by Metzler-Nolte et al.[23] for the coupling of a Ru^{II} complex to a PNA monomer. The formation of **2** was confirmed by mass spectrometry but all our attempts to purify the crude compound were unsuccessful despite intensive investigation of preparative column chromatography on silica gel with different eluents. The impurity present in **2** was confirmed to be the PNA backbone by both mass spectrometry and ^{1}H NMR spectroscopy. Peak integration of the resonances attributed to the *tert*-butyl moiety of the PNA backbone and **2** was used to establish that 33% of the crude product consisted of the PNA backbone, viz., ratio of PNA backbone/**2** = 1:3. The low conversion of **1** to **2** may be explained by unfavourable steric interactions between the bulky Ru^{II} complex, *tert*-butyl ester and fluorenylmethoxycarbonyl (Fmoc) protecting groups of the PNA backbone. The Ru^{II}-HBTU bulky adduct may also hinder the amine of the PNA backbone from attacking the carbonyl group, giving rise to low coupling efficiencies between **1** and the PNA backbone (see Hyperchem models of energy-minimized structure of **2** and **5** in the Supporting Information). The *tert*-butyl group protecting the carboxylic group in **2** was removed using a 1:1 mixture of TFA/CH_2Cl_2 with triethylsilane as the carbocation scavenger[38,39] to afford **M1** in 79% yield.

A similar series of reactions converted **1** to **M2** in good yield. Compound **1** was first converted into the Ru^{II}-succinimide derivative $[Ru(bpy)_2(Mebpy\text{-}OSu)]^{2+}$ (**3**), where Mebpy-OSu = 4′-methyl-2,2′-bipyridine-4-succinimide, as described previously.[40] Peek et al.[40] and Geiβer et al.[41–43] had attached unprotected amino acids to **3**. Thus, **3** was considered a suitable reactant for the attachment of an unprotected linker unit, 6-aminocaproic acid, to **1** to give **4**. With modifications to reported methods,[41–43] including higher temperature (120 °C) and longer reaction times

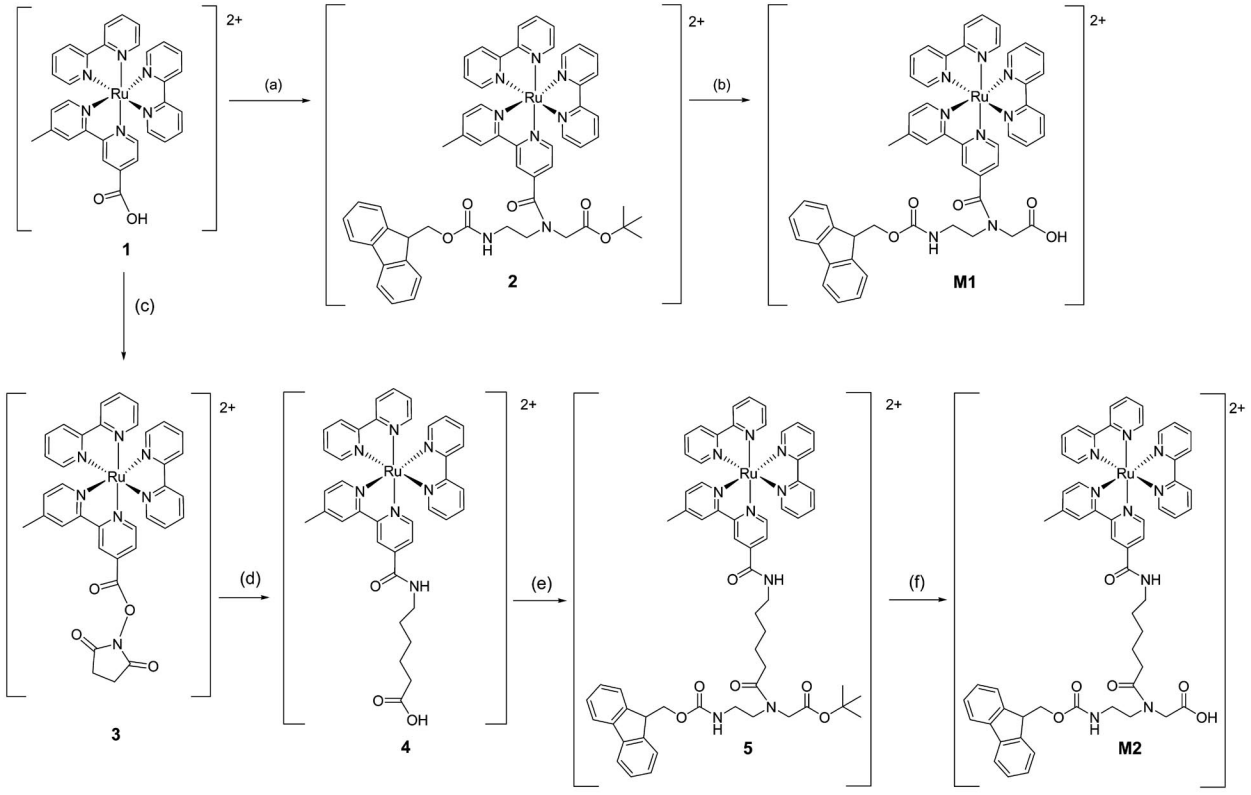

Scheme 1. Reagents and conditions: (a) *tert*-butyl *N*-[2-(*N*-9-fluorenylmethoxycarbonyl)aminoethyl]glycinate, HBTU, NEt_3, dry CH_3CN, 24 h, 11%; (b) TFA/CH_2Cl_2, 1:1, Et_3SiH, 15 h, 79%. (c) HOSu, DCC, dry CH_3CN, 6 h, 67% (d) 6-aminocaproic acid, dry CH_3CN, 24 h, 68%. (e) HBTU, NEt_3, dry CH_3CN, 24 h, 42% (f) TFA/CH_2Cl_2, 1:1, Et_3SiH, 24 h, 70%.

(24 h), **4** was obtained in 68% yield. The Ru^{II}-PNA ester **5** was synthesised from **4** by the coupling method used to prepare compound **2**. As for **2**, the purification of compound **5** by preparative column chromatography on both silica gel and alumina oxide using different eluents was unsuccessful. The presence of the PNA backbone was confirmed with mass spectrometry and ^1H NMR spectroscopy, which indicated that 23% of the crude product consisted of the PNA backbone., viz., ratio of PNA backbone/**5** = 2:9. The yield of **5** was much higher than that found for **2**. The alkyl chain appears to reduce interactions between the bulky Fmoc, *tert*-butyl moieties and the Ru^{II} complex (see Supporting Information). Cleavage of the *tert*-butyl ester in **5**, as for **2**, resulted in the final compound **M2** in 70%, yield.

Microanalysis confirmed the formation of the target complexes **4**, **M1** and **M2** (see Exp. Section). ESI-mass spectrometry of **2**, **4**, **5**, **M1** and **M2** gave signals with *m*/*z* values of 503.2, 370.6, 559.8, 475.1 and 531.2, respectively, corresponding to M^{2+}. The IR spectra of **4**, **M1** and **M2** all showed overlapping vibrations in the range 1635 cm^{-1} to 1655 cm^{-1} and 1715 cm^{-1} to 1720 cm^{-1} due to the carbonyl stretching mode within the amide and ester groups.

^1H-^1H COSY NMR spectroscopy enabled the assignment of each proton in the ^1H NMR spectra of **2**, **4**, **5**, **M1** and **M2**. Reaction of the activated ester, **3**, with the amine group of the 6-aminocaproic acid produced **4** whose ^1H NMR spectrum exhibited low frequency resonances due to the methylene units on the alkyl chain. Formation of **2** and **5**, from coupling between the PNA backbone and **1** and **4**, respectively, was confirmed by the presence of resonances at 1.36–1.40 ppm, assigned to the *tert*-butyl groups of the PNA backbone as mentioned previously.

Significant shifts in the resonances of some of the bipyridyl protons, in **2**, **4** and **5** were observed when compared with **1**.[44] In particular, the resonance attributed to the proton next to the carboxylic acid group in **1**, H3′, undergoes significant changes upon attachment to the PNA backbone and spacer group. A lower frequency shift of the H3′ resonance from 9.08 ppm into the region of 8.58–8.78 ppm is observed in going from **1** to **2**. Similar to **1**,[44] the H3′ resonances of **4** and **5** are observed at δ = 9.04 ppm and 9.07 ppm, respectively. In contrast to the conversion of **1** into **2**, little change in the position of the H3′ resonance is observed in going from **4** to **5**, due to the presence of the longer linker unit.

The presence of two rotamers in **2** was established by ^1H NMR spectroscopy, viz., two resonances for the bipyridyl methyl group were observed at δ = 2.46 ppm (minor) and 2.60 ppm (major). Peak integration of these resonances indicated that the rotamers were present in a ratio of 3:1 (major/minor). As for **2**, the spectrum of **5** exhibits two methyl groups at 2.60 (major) and 2.59 (minor) ppm arising from the presence of rotamers in a ratio of 3:2 (major/minor). Cleavage of the *tert*-butyl groups of **2** and **5** was confirmed by the absence of the *tert*-butyl group resonance,

Table 1. UV/Vis spectroscopic data obtained for 10 μM acetonitrile solutions of **1**, **4**, **M1** and **M2**.

Complex	λ_{max} [nm] (LC)	ε_{molar} [$M^{-1}cm^{-1}$] (LC)	λ_{max} [nm] (LC)	ε_{molar} [$M^{-1}cm^{-1}$] (LC)	λ_{max} [nm] (LC)	ε_{molar} [$M^{-1}cm^{-1}$] (LC)	λ_{max} [nm] (MLCT)	ε_{molar} [$M^{-1}cm^{-1}$] (MLCT)
1[44]	243	26800	254	23800	287	77600	453	14100
4	243	21800	254	21400	287	64700	453	13300
M1	243	26300	254	25900	287	71700	454	14600
M2	244	29800	254	35600	287	70200	454	14300
$[Ru(bpy)_3]^{2+}$[44]	241	21000	–	–	285	64700	451	11970

at around 1.35–1.40 ppm, in the ^1H NMR spectra of **M1** and **M2** (see Supporting Information). The remaining protons for **M1** and **M2** appeared at similar chemical shifts to those observed in the ^1H NMR spectra of **2** and **5**, respectively, except for the CH_2 protons closest to the carboxylate groups (CH_2-COOH) on the PNA unit. A chemical shift of + 0.12 ppm is observed for these CH_2 protons upon cleavage of the *tert*-butyl group for **M1**, while a shift of +0.29 ppm was observed for **M2**.

UV/Vis Spectra

The UV/Vis spectra of **1**, **4**, **M1** and **M2**, recorded in acetonitrile at 293 K, are compared in Table 1. The spectra of crude **2** and **5** were recorded under the same conditions (see Exp. Sect.), but the molar extinction coefficients are unreliable due to the presence of PNA monomer impurities. Analogous to **1** and $[Ru(bpy)_3]^{2+}$,[44] **4**, **M1** and **M2** exhibit strong absorption bands in the UV and visible regions of the electronic spectrum.

In the UV region, LC transitions ($\pi \rightarrow \pi^*$) of **4**, **M1** and **M2** were assigned on the basis of the positions of the absorption maxima and the molar extinction coefficients (see Table 1). In comparison to **1**, the spectrum of **4** showed slight decreases in the intensities of all LC bands, but no changes in the positions of the absorption maxima. This suggests a small effect of the alkyl spacer group on the energy levels of the bpy ligand. The position and intensity of LC transitions for **M1** and **M2** were similar to those for **1** and **4**, although **M2** exhibited slightly more intense bands than **4**. Intense bands found at ca. 205 nm, in the spectra of **M1** and **M2**, respectively are most likely due to the LC transition occurring within the PNA monomer backbone.

In the visible region, **2** and **5** displayed a high intensity absorption centred at 454 nm which is assigned to the MLCT, as in the case of $[Ru(bpy)_3]^{2+}$ and **1**,[44] and thymine-bound Ru^{II}-PNA monomer (453 nm).[23] Distinct bands observed at 453 nm for **4** and 454 nm for **M1** and **M2** are also assigned to the MLCT. As expected, attachment of the linker group followed by coupling of the PNA backbone to the metal complex **1** does not produce significant change in the positions of the MLCT bands and the absorption intensities of **4**, **M1** and **M2**.

Emission Spectroscopy

The emission spectra of acetonitrile solutions of **1**, **4**, **M1** and **M2** were recorded at 293 K following excitation at 450 nm (Figure S8, Supporting Information, and Table 2). Again, the spectra of **2** and **5** were affected by the presence of the impurity and, as a result, only their emission wavelengths are reliable. Consistent with the UV/Vis studies, **1**,[44] **2**, **4**, **5**, **M1** and **M2** exhibit similar emission behaviour (Figure 2) with maxima detected at 623, 631, 625, 633, 631, and 622 nm, respectively. These maxima are at slightly higher wavelengths (red-shifted) than observed for $[Ru(bpy)_3]^{2+}$ (615 nm) under the same conditions. This slight red shift is due to the lowering of the energy of the π^* orbital of the bipyridyl ring caused by conversion of the carboxylic acid to an amide group. Slight changes in the emission maxima and their intensities were observed when comparing **1** and **M1** and **4** and **M2**. The minor red shift in the emission maximum of **M1**, cf. **1**, suggests the lowering of the LUMO energy levels on the functionalised bpy ligand upon coupling to the PNA backbone. No corresponding change was observed for **M2**, cf. **4**, due to the presence of the alkyl spacer group. Notably, a decrease in the intensity of the emission is found on attachment of the PNA backbone to **1** and **4**.

Table 2. Summary of data obtained from emission spectra of complexes **1**, **4**, **M1** and **M2** (10 μM acetonitrile solutions) following excitation at 450 nm.

Complex	λ_{max} [nm]	I_s/I_{ref}	Φ_R
1[44]	623	0.99	0.060
4	625	1.22	0.060
M1	631	1.01	0.045
M2	622	1.03	0.047
$[Ru(bpy)_3]^{2+}$[44]	615	1.00	0.062

On the basis of the emission intensities obtained on excitation at 450 nm and the molar extinction coefficients derived from the absorption data, quantum yields (Φ_R) of **1**, **4**, **M1** and **M2** were determined in CH_3CN assuming that Φ_{ref} of the reference compound $[(Ru(bpy)_3]^{2+}$ is 0.062. The quantum yields of the series of complexes are listed in Table 2 and were calculated according to Equation (1) as adopted from previous work.[44,45]

$$\Phi_R = \Phi_{ref} (I_s A_{ref}/I_{ref} A_s) \quad (1)$$

(I_s and I_{ref} in Equation (1) correspond to the emission intensity calculated from the area under the emission spectrum of the sample and reference, respectively and A_s and A_{ref} refer to the absorbance of the sample and reference from the UV/Vis spectra, respectively.) The quantum yields of **1** and **4** are similar to that of $[Ru(bpy)_3]^{2+}$ (Table 2). However, **M1** and **M2** exhibit lower quantum yields than **1**,

4 and $[Ru(bpy)_3]^{2+}$, indicating that the insertion of the PNA backbone, by an amide linkage, may be affecting the triplet MLCT excited state from which energy transfer occurs.

Electrochemical Studies

Cyclic Voltammetry

Data obtained from cyclic voltammetric responses (Figure S9, Supporting Information) for oxidation of **M1** and **M2** and their precursors, **2**, **4** and **5** compounds **M1** and **M2** at a stationary platinum (Pt) electrode in acetonitrile (0.1 M nBu_4NPF_6) are summarised in Table S1. Voltammograms of the PNA backbone exhibited no oxidation processes in the potential range of 0–1400 mV vs. $Fc^{0/+}$ (Fc = ferrocene). Thus, the electrochemistry of the impure **2** and **5** at positive potentials can be readily interpreted. All compounds exhibit a single electrochemically (ΔE_p close to 60 mV) and chemically ($|I_p^{ox}/I_p^{red}|$ close to unity) reversible Ru^{II}/Ru^{III} one-electron oxidation process, analogous to the oxidation of $[Ru(bpy)_3]^{2+}$ to $[Ru(bpy)_3]^{3+}$, as summarised in Equation (2).[46]

$$[Ru^{II}(bpy)_3]^{2+} \rightleftharpoons [Ru^{III}(bpy)_3]^{3+} + e^- \quad (2)$$

The average of the oxidation E_p^{ox} and reduction E_p^{red} peak potentials, $(E_p^{ox} + E_p^{red})/2$, obtained from cyclic voltammograms provides a measure of the formal potential, E^0_f, for the Ru^{II}/Ru^{III} couple. E^0_f values determined this way for **M1** and **M2** were 907 mV and 895 mV vs. Fc/Fc^+, respectively, and similar to those for **1** (922 mV vs. $Fc^{0/+}$) and $[Ru(bpy)_3]^{2+}$ (888 mV vs. $Fc^{0/+}$) reported previously.[44] E^0_f values determined for **2**, **4** and **5** were 857 mV, 884 mV and 901 mV vs. $Fc^{0/+}$, respectively.

E^0_f for **2** is 31 mV and 85 mV less positive than $[Ru(bpy)_3]^{2+}$ and **1**, respectively. The difference can be attributed to the insertion of the PNA backbone. In contrast, **4** and **5** both exhibit similar E^0_f values that lie within the range of $[Ru(bpy)_3]^{2+}$ and **1**. Presumably, the linker unit, which draws the PNA backbone away from the metal, minimises any substituent effect.

The E^0_f value **for M1** lies nearer to those for **1** and $[Ru(bpy)_3]^{2+}$. The more positive value for **M1** compared to **2** is attributed to the conversion of the *tert*-butyl ester to the electron withdrawing carboxylic acid. **M2** has a similar potential (895 mV vs. $Fc^{0/+}$) to **1**, $[Ru(bpy)_3]^{2+}$, its precursors **4** and **5** and its derivative **M1**, as expected if the linker group minimises the effect of the PNA backbone on the Ru^{II} center.

The oxidation-peak currents (I_p) were found to be linearly dependent on the square root of the scan rate for all complexes, as expected, because the reversible processes are diffusion controlled. Use of the Randles–Sevcik relationship[47] gives diffusion-coefficient values of $(1.1 \pm 0.1) \times 10^{-5}$ $cm^2 s^{-1}$, $(9.2 \pm 0.1) \times 10^{-6}$ $cm^2 s^{-1}$ and $(9.6 \pm 0.1) \times 10^{-6}$ $cm^2 s^{-1}$ for **4**, **M1** and **M2**, respectively, which are similar to diffusion coefficients previously reported for **1** and $[Ru(bpy)_3]^{2+}$.[44,48] Ligand-based reduction processes were detected at negative potentials but are not discussed in this paper.

Rotated Disc Voltammetry

Platinum rotated-disc voltammetric experiments with **M1** and **M2**, gave rise to a sigmoidal-shaped curve for the $Ru^{II/III}$ redox couple (Figure 2 displays the data for **M1**). The half-wave potential ($E_{1/2}$) values (potential where the current is half the value ($I_L/2$) of the limiting current, I_L) for both monomers were found to be consistent with the E^0_f values derived from cyclic voltammetry, as expected for a reversible process. A small shift in $E_{1/2}$ was found at high rotation rates indicating that there is uncompensated ohmic IR_L drop at high current regimes.

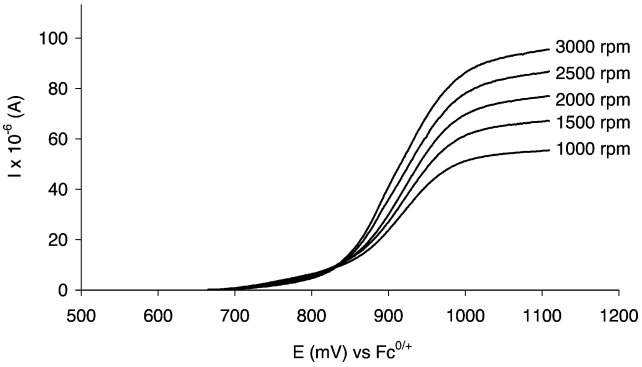

Figure 2. Platinum rotated-disc electrode voltammograms obtained for the oxidation of 0.64 mM **M1** in MeCN (0.1 M nBu_4NPF_6); rotation rates of 1000–3000 rpm and scan rate of 10 mV s^{-1}.

A high level of reproducibility of the rotated-disc electrode voltammograms was obtained only at rotation rates above 1000 rpm and 2000 rpm for **M1** and **M2**, respectively. A plot of the limiting current, i_L, vs. the square root of the angular velocity, $\omega^{1/2}$ (over the range of 1000 or 2000–3000 rpm) was linear for both compounds, as expected for a mass transport controlled process. The slope of this plot and use of the Levich equation[49] gave a diffusion coefficient values for **M1** and **M2** of $(1.0 \pm 0.1) \times 10^{-5}$ $cm^2 s^{-1}$ and $(9.8 \pm 0.1) \times 10^{-6}$ $cm^2 s^{-1}$ and in good agreement with values obtained from cyclic voltammetry. The origin of the prewave (Figure 2) and lower reproducibility at slow rotation rates may be associated with a small level of surface interaction.

Conclusions

Syntheses of two new monomeric PNA derivatives incorporating redox and photoactive polypyridyl-ruthenium(II) complexes have been developed. UV/Vis and emission spectra measurements on these monomers **M1** and **M2** and their respective intermediates, **1** **2**, **4** and **5** show similar behaviour to those that have been reported previously by our group and by Metzler-Nolte and co-workers.[23,32,44] Electrochemical measurements showed that all complexes give rise to a reversible one-electron Ru^{II}/Ru^{III} process. The in-

sertion of a linker group between the metal center and the PNA unit in **M2** relative to **M1** *only* has a small effect on the luminescence and electrochemistry of the ruthenium complex.

Experimental Section

Materials: Unless otherwise specified, reagents and chemicals were purchased from the commercial sources and used without further purification. In the synthetic work, solvents were used as received or dried with 4-Å molecular sieves or by a literature procedure in the case of CH_3CN.[50] *tert*-Butyl *N*-[2-(*N*-9-fluorenylmethoxycarbonyl)aminoethyl]-*N*-[(thymin-1-yl)acetyl]glycinate was synthesised by the procedure of Thomson et al.[38] The analytical data were in agreement with that reported previously.[38] Prior to use in coupling reactions, compound **1** was acidified to pH 1 using HPF_6 (60%, Aldrich) to obtain the fully protonated species. HPF_6 was also used to convert the nitrate salts of the *tert*-butyl Ru^{II}-PNA adducts to the corresponding hexafluorophosphates. Complexes were dissolved in HPLC-grade CH_3CN (Aldrich) for spectroscopic and electrochemical characterisation. High-purity nitrogen gas was used directly from the reticulated system. De-ionised water was distilled prior to use. Tetrabutylammonium hexafluorophosphate ($n$$Bu_4NPF_6$, Fluka) was recrystallised[51] prior to use as the electrolyte in electrochemical studies.

Instrumentation and Methods: ^1H NMR and ^1H-^1H COSY spectra were recorded in deuterated solvents using an Avance DRX400 Bruker spectrometer at 30 °C. The chemical shifts δ are reported in ppm (parts per million). Tetramethylsilane (TMS) or the residual solvent peaks have been used as an internal reference. The abbreviations for the peak multiplicities are as follows: s (singlet), d (doublet), dd (doublet of doublets), t (triplet), q (quartet), m (multiplet) and br (broad). 2D experiments were conducted and analysed with the aid of XWinNMR software. Infrared spectra were recorded with a Perkin–Elmer 1600 series FTIR spectrophotometer at 4 cm^{-1} resolution on samples doped in KBr pellets. UV/Vis spectra were recorded with a Varian Cary 300 Biospectrometer. Emission spectra were obtained following excitation at 450 nm with a Varian Fluorescence spectrometer equipped with a 250-W xenon lamp as the excitation source. Emission spectra are corrected for PMT response. Both UV/Vis and emission spectra were measured in acetonitrile solution at room temperature of (20 ± 2) °C in 1-cm quartz cuvettes using 10 μM concentrations of the complex. CHN analyses were performed by the Campbell Microanalytical Services, University of Otago, Dunedin, NZ. Low-resolution electrospray mass spectra were recorded with a Micromass Platform II Quadrupole Mass Spectrometer fitted with an electrospray source. High-resolution accurate mass spectra were recorded with a Bruker BioApex II 47e FT-ICR MS fitted with an Analytica Electrospray Source. Samples were introduced by a syringe pump at a rate of 1 μL/min and the capillary voltage was at 200 V. Thin-layer chromatography (TLC) was performed using silica gel 60 F-254 (Merck) plates followed by preparative column chromatography on silica gel.

Electrochemical Measurements: Cyclic voltammetric measurements were performed in acetonitrile at scan rates in the 0.002–1 $V s^{-1}$ range using a BAS 100B (Bioanalytical Systems) electrochemical workstation. Rotating-disc voltammetry at rates from 500–3000 rpm utilized a platinum disk working electrode (0.071 cm^2) and rotations were carried out with a Metrohm 628–10 system. Oxygen was removed from the acetonitrile solutions before commencing electrochemical experiments by purging the solutions with high purity nitrogen for at least 10 min. A typical three electrode cell was employed which comprised a platinum working electrode (area = 0.0079 cm^2 and 0.071 cm^2 for cyclic voltammetry and rotating disk voltammetry, respectively), a large surface area Pt counter electrode and an Ag/Ag^+ (0.1 M $AgNO_3$ in CH_3CN) reference electrode. The potential of the Ag/Ag^+ reference electrode was calibrated frequently against that of ferrocene/ferrocinium (Fc/Fc^+) redox couple by monitoring the reversible potential for oxidation of ferrocene (Fc) under the same conditions used for the voltammetry of the ruthenium(II) complexes. All electrochemical experiments were carried out at (20 ± 2)°C inside a Faraday cage under nitrogen and with 0.1 M $n$$Bu_4NPF_6$ as the supporting electrolyte. The working electrodes were polished with an aqueous aluminium oxide slurry (0.3 μM), then rinsed with acetone and dried before each voltammetric experiment.

Synthesis

[Ru(bpy)$_2$(Mebpy-COOH)](PF$_6$)$_2$ (1) and [Ru(bpy)$_2$(Mebpy-OSu)](PF$_6$)$_2$ (3): Compounds **1** and **3** were prepared according to literature methods.[37,52] The ^1H NMR spectra, mass spectroscopy and IR spectra were in agreement with the literature reports.[37,52]

[Ru(bpy)$_2$(Mebpy-PNA-OC(CH$_3$)$_3$)](PF$_6$)$_2$ (2): [Ru(bpy)$_2$(Mebpy-COOH)](PF$_6$)$_2$ (**1**) (0.23 g, 1.10 mmol) was dissolved in dry CH_3CN (3.0 mL) under nitrogen. 2-(1-*H*-Benzotriazol-1-yl)-1,1,3,3-tetramethyluronium hexafluorophosphate (HBTU) (0.43 g, 1.10 mmol) and triethylamine (0.15 mL, 1.10 mmol) was added to this solution. The solution was stirred for 15 min at room temperature prior to the addition of *tert*-butyl-*N*-[2-(*N*-9-fluorenylmethoxycarbonyl)aminoethyl]glycine (0.59 g, 1.50 mmol). The resulting solution was stirred overnight and a saturated brine solution (15 mL) was then added. The product was extracted with nitromethane (25 mL × 2) and the organic layer was then successively washed with 2 M $HCl_{(aq.)}$ (15 mL × 2), a saturated aqueous solution of $NaHCO_3$ (20 mL × 2) and water (25 mL × 2). The solvent of the organic layer was removed under vacuum to give a red solid. The crude product was purified by column chromatography on silica gel using either an increasing gradient from $MeOH/CH_2Cl_2$, 4:96 (v/v) to $MeOH/CH_2Cl_2$ 6:94 (v/v) or a CH_3CN/H_2O/saturated KNO_3, 80:20:1 solution (v/v/v) as the eluent. The first coloured band was collected and removal of the solvent by rotary evaporation gave the desired product together with a minor impurity. Attempts to separate the desired product from the impurity by further column chromatography with various eluents were unsuccessful. The actual yield of **2** was determined by the ratio of the PNA backbone to **2** in the crude product found from peak integration of the *tert*-butyl group (3:9). Crude yield 0.21 g, 16%, actual yield based on analysis of ^1H NMR spectra, 0.14 g, 11%. Selected IR bands (KBr): $\tilde{\nu}$ = 2924 (m), 1718 (m), 1638 (m), 1560 (w), 1522 (m), 1465 (m), 1447 (m), 1369 (m), 1236 (m), 1155 (m), 841 (m), 761 (m), 741 (w) cm^{-1}. UV/Vis spectrum (CH_3CN): λ_{max} (ε_{max}, $M^{-1} cm^{-1}$) = 207 (53700), 246 (30300), 255 (37400), 288 (52700), 422 (6100), 454 (10000) nm. ^1H NMR spectrum ([D$_6$]acetone): δ = 1.41 (min) and 1.47 (maj) [rotamers, s, 9 H, O-C-(CH_3)$_3$], 2.38 (maj) and 2.43 (min) (rotamers, s, 3 H, CH_3bpy-COOH), 3.15–3.30 (rotamers, m, 2 H, NH-CH_2-CH$_2$), 3.45–3.70 (rotamers, m, 2 H, NH-CH$_2$-CH_2), 3.87–4.02 (rotamers, m, 2 H, CH Fmoc-CH_2O), 4.28 [rotamers, m, 2 H, N-CH_2-COOC(CH$_3$)$_3$], 4.37 (rotamers, m, 1 H, C*H* Fmoc), 6.41 (min) and 6.46 (maj) (rotamers, br. s, 1 H, CH$_2$-N*H*-COO), 7.09–7.23 (m, 3 H, H5′ and 2 × C*H* Fmoc aromatic), 7.26–7.43 (m, 6 H, H11, 11′, 16, 16′ and 2 × C*H* Fmoc aromatic), 7.46–7.53 (m, 3 H, H6′ and 2 × C*H* Fmoc aromatic), 7.64–7.67 (d, ^3J = 5.8 Hz, 1 H, H6), 7.81–8.25 (m, 11 H, H5, 10, 10′, 12, 12′, 15 15′, 17, 17′ and 2 × C*H* Fmoc aromatic), 8.56–8.78 (m, 6 H, H3, 3′, 9, 9′, 14 and 14′) ppm. ESI-MS: m/z (%) = 503.2 (100) [(M)$^{2+}$], 475.2

(28) $[M - C(CH_3)_3]^{2+}$. HR-ESI mass spectrum (MeOH): found 503.1551; calcd. for $[C_{55}H_{52}N_8O_5Ru]/z$ 503.1552.

$[Ru(bpy)_2$(Mebpy-PNA-OH)$](PF_6)_2$ (M1): Compound **2** (0.18 g, 0.14 mmol) was dissolved in dichloromethane (3.5 mL) and trifluoroacetic acid (2.3 mL) and triethylsilane (0.6 mL) were added to this solution. The resulting solution was stirred for 6 h at room temperature. Removal of the trifluoroacetic acid and dichloromethane under vacuum resulted in a viscous dark red oil. This oil was purified by column chromatography on silica using CH_3CN/H_2O/saturated KNO_3, 80:20:1 (v/v/v) as the eluent, followed by a gradual change to 60:40:1 (v/v/v) to elute the last band. The solvent was removed in vacuo and the residue suspended in a minimal amount of acetonitrile. The insoluble KNO_3salt was removed by filtration and the filtrate was evaporated to dryness to give **M1**. The residue was then sonicated in water (10 mL) for 5 min to dissolve the solid. A 60% aqueous solution of HPF_6 was added until a pH of 1 was attained. The precipitate was collected by filtration and triturated with ether to afford the desired product. Yield 0.13 g, 79%. $C_{55}H_{64}F_{12}N_8O_3P_2Ru$: calcd. C 48.1, H 4.7, N 8.2; found C 47.9, H 4.8, N 8.4. Selected IR bands (KBr): $\tilde{\nu}$ = 2926 (w), 1701 (w), 1636 (m), 1560 (w), 1508 (w), 1452 (m), 1384 (s), 1209 (m), 933 (w), 821 (w), 769 (w) cm^{-1}. UV/Vis spectrum (CH_3CN): λ_{max} (ε_{max}, $M^{-1}cm^{-1}$) = 243 (26300), 254 (25900), 287 (71700), 422 (13800), 454 (14600) nm. ^1H NMR spectrum ([D$_6$]acetone): δ = 2.41 (maj) and 2.47 (min) (rotamers, s, 3 H, C*H*$_3$bpy-COOH), 3.32–3.34 (rotamers, m, 2 H, NH-C*H*$_2$-CH$_2$), 3.45–3.52 (rotamers, m, 2 H, NH-CH$_2$-C*H*$_2$), 3.94–4.05 (rotamers, m, 2 H, CH Fmoc-C*H*$_2$O), 4.20 (s, 1 H, C*H* Fmoc), 4.32–4.36 (rotamers, m, 1 H, N-C*H*$_2$-COOH), 6.41 (min) and 6.64 (maj) (rotamers, br. s, 1 H, CH$_2$-N*H*-COO), 7.23–7.39 (m, 2 H, 2 × C*H* Fmoc aromatic), 7.39 (d, ^3J = 5.9 Hz, 1 H, H5′), 7.55–7.57 (m, 6 H, H11, 11′, 16, 16′ and 2 × C*H* Fmoc aromatic), 7.78–7.93 (m, 3 H, H6′ and 2 × C*H* Fmoc aromatic), 7.95–8.01 (m, 5 H, H5,12,12′,17,17′), 8.02 (d, ^3J = 5.8 Hz 1 H, H6), 8.16–8.24 (m, 6 H, H10,10′,15,15′ and 2 × C*H* Fmoc aromatic), 8.79–8.84 (m, 5 H, H3,9,9′,14,14′), 9.09 (s, 1 H, H3′) ppm. ESI-MS: *m*/*z* (%) = 475.2 (14) $[M]^{2+}$, 486.2 (100) $[M - H + Na]^{2+}$. HR-ESI mass spectrum (MeOH): found 475.0078; calcd. for $[C_{51}H_{44}N_8O_5Ru]/z$ 475.1224.

$[Ru(bpy)_2$(Mebpy-$(CH_2)_4$-COOH)$](PF_6)_2$ (4): 6-Aminocaproic acid (0.05 g, 0.41 mmol) was dissolved in dimethylformamide (3 mL). $[Ru(bpy)_2$(Mebpy-OSu)$](PF_6)_2$[40] (**3**, 0.21 g, 0.21 mmol) was added to this stirring suspension. This mixture was refluxed at 160 °C for 24 h. Most of the solvent was then removed in vacuo leaving a wet dark orange residue, which was suspended in dichloromethane (10 mL) and filtered. The filtrate was then extracted with a 10 mM aqueous solution of NH_4PF_6 (2 × 15 mL). The combined aqueous phases were extracted with dichloromethane (1 × 20 mL). The organic phases were combined and dried with anhydrous $MgSO_4$ followed by filtration to remove the drying agent. The filtrate was concentrated under vacuum until precipitation was observed. The mixture was left to stand overnight at 4 °C to allow further precipitation of the product. The pure product was collected via filtration, washed with diethyl ether (3 × 10 mL) and dried in air to give an orange solid. Yield 0.16 g, 68%. $C_{38}H_{37}F_{12}N_7O_3P_2Ru$: calcd. C 44.3, H 3.6, N 9.5; found C 44.4, H 3.9, N 9.4. Selected IR bands (KBr): $\tilde{\nu}$ = 2361 (m), 1654 (m), 1637 (w), 1560 (w), 1449 (m), 1099 (w br), 842 (s), 669 (w) cm^{-1}. UV/Vis spectrum (CH_3CN): λ_{max} (ε_{max}, $M^{-1}cm^{-1}$) = 243 (21800), 254 (21400), 287 (64700), 423 (12100), 453 (13300) nm. ^1H NMR spectrum ([D$_6$]acetone): δ = 1.26–1.32 [m, 2 H, NH-CH$_2$-CH$_2$-C*H*$_2$ (linker)], 1.33–1.43 [m, 2 H, NH-C*H*$_2$-CH$_2$ (linker)], 1.54–1.62 [m, 4 H, NH-CH$_2$-C*H*$_2$ (linker) and HOOC-CH$_2$-C*H*$_2$ (linker)], 2.25 (m, 2 H, HOOC-C*H*$_2$-CH$_2$), 2.58 (major) and 2.59 (minor) [rotamers, s, 3 H, (bpy-COOH)-C*H*$_3$], 5.27 (minor) and 5.58 (major) (rotamers, br. s, Mebpy-CO-N*H*), 7.27 (d, ^3J = 5.9 Hz, 1 H, H5), 7.41–7.56 (m, 4 H, H11,11′,16,16′), 7.78–7.89 (m, 2 H, H6,6′), 7.88–8.00 (m, 4 H, 12, 12′, 17 and 17′), 8.02 (d, ^3J = 6.1 Hz, 1 H, H5′), 8.09–8.20 (m, 4 H, H10,10′,15,15′), 8.72–8.81 (m, 5 H, H3′,9,9′,14 and 14′), 9.04 (s, 1 H, H3) ppm. ESI-MS: *m*/*z* (%) = 370.6 (100) $[M]^{2+}$.

$[Ru(bpy)_2$(Mebpy-$(CH_2)_4$-PNA-OC$(CH_3)_3$)$](PF_6)_2$ (5): Compound **5** was prepared in the same manner as **2**, but using **4** as a precursor (0.53 g, 0.51 mmol), HBTU (0.20 g, 0.52 mmol), *tert*-butyl-*N*-[2-(*N*-9-fluorenylmethoxycarbonyl)aminoethyl]glycine (0.30 g, 0.75 mmol) and triethylamine (0.07 mL, 0.55 mmol). The product was obtained as a dark orange solid. Attempts to separate the desired product from an impurity by a second level of column chromatography and using various eluents were unsuccessful. The yield of **5** was determined by the ratio of the PNA backbone to **5** in the crude product found from peak integration of the *tert*-butyl group (2:9). Crude yield 0.40 g, 54%, actual yield based on ^1H NMR interpretation, 0.31 g, 42%. Selected IR bands (KBr): $\tilde{\nu}$ = 2932 (w), 1717 (m), 1648 (m), 1542 (m), 1465 (w), 1384 (m), 1154 (m), 843 (s) cm^{-1}. UV/Vis spectrum (CH_3CN): λ_{max} (ε_{max}, $M^{-1}cm^{-1}$) = 207 (58500), 255 (20100), 288 (43400), 424 (6200), 454 (8800) nm. ^1H NMR spectrum ([D$_6$]acetone): δ = 1.18 [m, 2 H, NH-CH$_2$-CH$_2$-C*H*$_2$ (linker)], 1.41 [m, 4 H, NH-C*H*$_2$-CH$_2$ (linker) and NH-CH$_2$-C*H*$_2$ (linker)], 1.47 (min) and 1.49 (maj) [rotamers, s, 9 H, O-C-(C*H*$_3$)$_3$], 2.41–2.46 [rotamers, m, 2 H, HNOC-CH$_2$-C*H*$_2$ (linker)], 2.59 (maj) and 2.60 (min) (rotamers, s, 3 H, C*H*$_3$bpy-COOH), 3.18 and 3.20 [rotamers, m, 2 H, HNOC-C*H*$_2$-CH$_2$ (linker)], 3.54–3.65 [m, 4 H, NH-C*H*$_2$-CH$_2$ (PNA backbone) and NH-CH$_2$-C*H*$_2$ (PNA backbone)], 3.88 and 4.02 [rotamers, m, 2 H, CH Fmoc-C*H*$_2$O (PNA backbone)], 4.17–4.22 [m, 2 H, N-C*H*$_2$-COOC(CH$_3$)$_3$ (PNA backbone)], 4.33 [m, 1 H, C*H* Fmoc (PNA backbone)], 5.29 (maj), 6.52 (min), 6.63 (min) and 7.08 (min) [rotamers, br. s, 1 H, CH$_2$-N*H*-COO (PNA backbone)], 7.32–7.41 (m, 7 H, H5′, 11, 11′, 16, 16′, 2 × C*H* Fmoc aromatic), 7.52–7.63 (m, 5 H, H5,12,12′,17,17′), 7.67 (d, ^3J = 6.0 Hz, 1 H, H6), 7.81–7.89 (m, 4 H, 4 × C*H* Fmoc aromatic), 8.20 (m, 4 H, H10,10′,15,15′), 8.79–8.86 (m, 5 H, H3,9,9′,14,14′), 9.07 (s, 1 H, H3) ppm. ESI-MS: *m*/*z* (%) = 559.8 (45) $[M]^{2+}$. HR-ESI mass spectrum (MeOH): found 559.6982; calcd. for $[C_{61}H_{65}N_9O_6Ru]/z$ 559.6973.

$[Ru(bpy)_2$(Mebpy-$(CH_2)_4$-PNA-OH)$](PF_6)_2$ 5H_2O (M2): M2 was obtained as a light orange solid in the same manner as **M1**, but using **5** (0.37 g, 0.26 mmol) dissolved in dichloromethane (3.0 mL), trifluoroacetic acid (2.0 mL) and triethylsilane (0.4 mL). Yield 0.35 g, 70%. $C_{57}H_{65}F_{12}N_9O_{11}P_2Ru$: calcd. C 47.4, H 4.5, N 8.7; found C 47.7, H 4.3, N 8.9. Selected IR bands (KBr): $\tilde{\nu}$ = 2934 (w), 1718 (m), 1654 (m), 1542 (m), 1466 (m), 1447 (m), 1239 (w), 842 (s) cm^{-1}. UV/Vis spectrum (CH_3CN): λ_{max} (ε_{max}, $M^{-1}cm^{-1}$) = 205 (84200), 244 (29800), 254 (35600), 287 (70200), 424 (11000), 454 (14300) nm. ^1H NMR spectrum ([D$_6$]acetone): δ = 1.38 [m, 2 H, NH-CH$_2$-CH$_2$-C*H*$_2$ (linker)], 1.60 [m, 4 H, NH-C*H*$_2$-CH$_2$ (linker) and NH-CH$_2$-C*H*$_2$ (linker)], 2.25 and 2.41 [rotamers, m, 2 H, HNOC-CH$_2$-C*H*$_2$ (linker)], 2.57 (min) and 2.59 (maj) (rotamers, s, 3 H, C*H*$_3$bpy-COOH), 3.11 and 3.23 [rotamers, m, 2 H, HNOC-C*H*$_2$-CH$_2$ (linker)], 3.42–3.47 [m, 4 H, NH-C*H*$_2$-CH$_2$ (PNA backbone) and NH-CH$_2$-C*H*$_2$ (PNA backbone)], 3.66 and 4.04 [rotamers, m, 1 H, C*H* Fmoc (PNA backbone)], 4.17 and 4.29 [rotamers, s, 2 H, N-C*H*$_2$-COOH (PNA backbone)], 5.23 (maj), 6.46 (min), 6.66 (min) and 7.11 (min) [rotamers, br. s, 1 H, CH$_2$-N*H*-COO (PNA backbone)], 7.29 (m, 1 H, H5′), 7.36–7.41 (m, 2 H, 2 × C*H* Fmoc aromatic), 7.55–7.62 (m, 6 H, H11,11′,16,16′ and 2 × C*H* Fmoc aromatic), 7.83–7.87 (m, 3 H, H6′ and 2 × C*H* Fmoc aromatic), 8.02–8.07 (m, 5 H, H5,12,12′,17,17′), 8.09 (d, ^3J = 6.0 Hz, 1 H, H6), 8.20 (m, 6 H, H10,10′,15,15′ and 2 × C*H* Fmoc aro-

matic), 8.79 (m, 5 H, H3,9,9′,14,14′), 9.09 (s, 1 H, H3) ppm. ESI-MS: *m*/*z* (%) = (100) 561.1 [M^{2+}]. HR-ESI mass spectrum (MeOH): found 531.6660; calcd. for [$C_{57}H_{55}N_9O_6Ru$]/*z* 531.6661.

Supporting Information (see also the footnote on the first page of this article): Representative examples of ^{1}H NMR spectra of **2**, **4**, **5**, **M1** and **M2**; hyperchem models of **2** and **5**; luminescence spectra of **1**, **4**, **M1**, **M2**; cyclic voltammograms of **M1** and **M2**; and summary of electrochemical data obtained by cyclic voltammetry for **2**, **4**, **5**, **M1** and **M2**.

Acknowledgments

The authors gratefully acknowledge financial support of this work by the Australian Research Council through the Australian Centre for Electromaterials Science (ACES), the Australian Discovery Program and the Federation Fellowship Scheme (to A. M. B.). N. N. is the recipient of a Monash University Departmental Scholarship.

[1] P. E. Nielsen, M. Egholm, R. H. Berg, O. Buchardt, *Science* **1991**, *254*, 1497.
[2] P. E. Nielsen, M. Egholm, in *Peptide Nucleic Acids, Protocols and Applications* (Eds.: P. E. Nielsen, M. Egholm), Horizon Scientific Press, Wymondham, UK, **1999**, pp. 1.
[3] R. P. Stock, A. Olvera, R. Sanchez, A. Saralegui, S. Scarfi, R. Sanchez-Lopez, M. A. Ramos, L. C. Boffa, U. Benatti, A. Alagon, *Nat. Biotechnol.* **2001**, *19*, 231.
[4] M. Pooga, U. Soomets, M. Hällbrink, A. Valkana, K. Saar, K. Rezaei, U. Kahl, J.-X. Hao, X. J. Xu, Z. Wiesenfeld-Hallin, T. Hökfelt, T. Bartfai, U. Langel, *Nat. Biotechnol.* **1998**, *16*, 857.
[5] B. M. Tyler, K. Jansen, D. J. McCormick, C. L. Douglas, M. Boules, J. A. Stewart, L. Zhao, B. Cusak, A. Fauq, E. Richelson, *Proc. Natl. Acad. Sci. USA* **1999**, *96*, 7053.
[6] J. J. Turner, S. Jones, M. M. Fabani, G. Ivanova, A. A. Arzumanov, M. J. Gait, *Blood Cells, Molecules Diseases* **2007**, *38*, 1.
[7] T. Shiraishi, P. E. Nielsen, *FEBS Lett.* **2006**, *580*, 1451.
[8] L. Chiarantini, A. Cerasi, A. Fraternale, E. Millo, U. Benatti, K. Sparnacci, M. Laus, M. Ballestri, L. Tondelli, *J. Controlled Release* **2005**, *109*, 24.
[9] R. Sanchez, A. Saralegui, A. Olivos-Garcia, C. Scapolla, G. Damonte, R. Sanchez-Lopez, A. Alagon, R. P. Stock, *Experimental Parasitology* **2005**, *109*, 241.
[10] B. A. Janowski, J. Hu, *Nat. Protoc.* **2006**, *1*, 436.
[11] B. A. Janowski, K. Kaihatsu, K. E. Huffman, J. C. Schwartz, R. Ram, D. Hardy, C. R. Mendelson, D. R. Corey, *Nat. Chem. Biol.* **2005**, *1*, 210.
[12] J. Hu, D. R. Corey, *Biochemistry* **2007**, *46*, 7581.
[13] G. Cutrona, L. C. Boffa, M. R. Mariani, S. Matis, G. Damonte, E. Millo, S. Roncella, M. Ferrarini, *Oligonucleotides* **2007**, *17*, 146.
[14] L. C. Boffa, G. Cutrona, M. Cilli, S. Matis, G. Damonte, M. R. Mariani, E. Millo, M. Moroni, S. Roncella, F. Fedeli, M. Ferrarini, *Cancer Gene Ther.* **2007**, *14*, 220.
[15] J. Wang, in *Peptide Nucleic Acids, Protocols and Applications* (Eds.: P. E. Nielsen, M. Egholm), Horizon Scientific Press, Wymondham, UK, **1999**, pp. 155.
[16] J. Wang, E. Palecek, P. E. Nielsen, G. Rivas, X. Cai, H. Shiraishi, N. Dontha, D. Luo, P. A. M. Farias, *J. Am. Chem. Soc.* **1996**, *118*, 7667.
[17] J. Wang, *Biosens. Bioelectron.* **1998**, *13*, 757.
[18] F. Le Floch, H.-A. Ho, P. Harding-Lepage, M. Bédard, R. Neagu-Plesu, M. Leclerc, *Adv. Mater.* **2005**, *17*, 1251.
[19] D. R. van Staveren, N. Metzler-Nolte, *Chem. Rev.* **2004**, *104*, 5931.
[20] J. H. R. Tucker, S. R. Collinson, *Chem. Soc. Rev.* **2002**, *31*, 147.
[21] G. Gasser, L. Spiccia, *J. Organomet. Chem.* **2008**, *693*, 2478.
[22] G. Gasser, M. J. Belousoff, A. M. Bond, L. Spiccia, *J. Org. Chem.* **2006**, *71*, 7565.
[23] A. Hess, N. Metzler-Nolte, *Chem. Commun.* **1999**, 885.
[24] R. H. E. Hudson, G. Li, J. Tse, *Tetrahedron Lett.* **2002**, *43*, 1381.
[25] C. Baldoli, P. Cerea, C. Giannini, E. Licandro, C. Rigamonti, S. Maiorana, *Synlett* **2005**, *13*, 1984.
[26] C. Baldoli, L. Falciola, E. Licandro, S. Maiorana, P. Mussini, P. Ramani, C. Rigamonti, G. Zinzalla, *J. Organomet. Chem.* **2004**, *689*, 4791.
[27] C. Baldoli, C. Giannini, E. Licandro, S. Maiorana, G. Zinzalla, *Synlett* **2004**, *6*, 1044.
[28] C. Baldoli, S. Maiorana, E. Licandro, G. Zinzalla, D. Perdicchia, *Org. Lett.* **2002**, *4*, 4341.
[29] C. Baldoli, C. Rigamonti, S. Maiorana, E. Licandro, L. Falciola, P. R. Mussini, *Chem. Eur. J.* **2006**, *12*, 4091.
[30] G. Gasser, N. Hüsken, S. D. Köster, N. Metzler-Nolte, *Chem. Commun.* **2008**, 3675.
[31] A. Maurer, H.-B. Kraatz, N. Metzler-Nolte, *Eur. J. Inorg. Chem.* **2005**, 3207.
[32] J. C. Verheijen, G. A. van der Marel, J. H. van Boom, N. Metzler-Nolte, *Bioconjuguate Chem.* **2000**, *11*, 741.
[33] P. Amit, R. M. Watson, P. Lund, Y. Xing, K. Burke, Y. He, E. Borguet, C. Achim, W. Waldeck, *J. Phys. Chem. C* **2008**, *112*, 7233.
[34] R. M. Franzini, R. M. Watson, G. K. Patra, R. M. Breece, D. L. Tierney, M. P. Hendrich, C. Achim, *Inorg. Chem.* **2006**, *45*, 9798.
[35] D.-L. Popescu, T. J. Parolin, C. Achim, *J. Am. Chem. Soc.* **2003**, *125*, 6354.
[36] R. M. Watson, Y. A. Skorik, G. K. Patra, C. Achim, *J. Am. Chem. Soc.* **2005**, *127*, 14628.
[37] B. M. Peek, G. T. Ross, S. W. Edwards, G. J. Meyer, T. J. Meyer, B. W. Erickson, *Int. J. Pept. Protein Res.* **1991**, *38*, 114.
[38] S. A. Thomson, J. A. Josey, R. Cadilla, M. D. Gaul, C. F. Hassman, M. J. Luzzio, A. J. Pipe, K. L. Reed, D. J. Ricca, *Tetrahedron* **1995**, *51*, 6179.
[39] A. Mehta, R. Jaouhari, T. J. Benson, K. T. Douglas, *Tetrahedron Lett.* **1992**, *33*, 5441.
[40] B. M. Peek, G. T. Ross, S. W. Edwards, G. J. Meyer, T. J. Meyer, B. W. Erickson, *Int. J. Pep. Protein Res.* **1991**, *38*, 114.
[41] B. Geiβer, R. Alsfasser, *Dalton Trans.* **2003**, 612.
[42] B. Geiβer, R. Alsfasser, *Inorg. Chim. Acta* **2003**, *348*, 179.
[43] B. Geiβer, A. Ponce, R. Alsfasser, *Inorg. Chem.* **1999**, *38*, 2030.
[44] N. Nickita, M. J. Belousoff, A. I. Bhatt, A. M. Bond, G. B. Deacon, G. Gasser, L. Spiccia, *Inorg. Chem.* **2007**, *46*, 8638.
[45] M. Zhou, G. P. Robertson, J. Roovers, *Inorg. Chem.* **2005**, *44*, 8317.
[46] A. M. Bond, G. B. Deacon, J. Howitt, D. R. MacFarlane, L. Spiccia, G. Wolfbauer, *J. Electrochem. Soc.* **1999**, *146*, 648.
[47] A. J. Bard, L. R. Faulkner, *Electrochemical Methods, Fundamentals and Application*, Second ed., Brisbane, Australia, **2001**.
[48] M. R. McDevitt, A. W. Addison, *Inorg. Chim. Acta* **1993**, *204*, 141.
[49] V. G. Levich, *Physicochemical Hydrodynamics* **1962**, *Prentice-Hall, Englewood Cliffs, New Jersey.*
[50] W. L. F. Armarego, D. D. Perrin, *Purification of Laboratory Chemicals*, 4th Edition ed., Butterworth-Heinemann, Oxford (UK), **1996**.
[51] A. J. Fry in *Laboratory Techniques in Electroanalytical Chemistry* (Eds.: T. Kissinger, W. R. Heineman), 2nd ed., Marcel Dekker, New York, **1996**, pp. 469.
[52] N. Nickita, G. Gasser, P. Pearson, L. Y. Goh, A. M. Bond, G. B. Deacon, L. Spiccia, *Inorg. Chem.* **2009**, 48, 68.

Received: December 28, 2008
Published Online: March 31, 2009

